Ain Shams Engineering Journal (2017) 8, 277–294

Ain Shams University
Ain Shams Engineering Journal
www.elsevier.com/locate/asej
www.sciencedirect.com

ENGINEERING PHYSICS AND MATHEMATICS

Computational study of Jeffrey's non-Newtonian fluid past a semi-infinite vertical plate with thermal radiation and heat generation/absorption

S. Abdul Gaffar [a,*], V. Ramachandra Prasad [b], E. Keshava Reddy [a]

[a] Department of Mathematics, Jawaharlal Nehru Technological University Anantapur, Anantapuramu, India
[b] Department of Mathematics, Madanapalle Institute of Technology and Science, Madanapalle 517325, India

Received 7 October 2015; revised 13 August 2016; accepted 2 September 2016
Available online 19 October 2016

KEYWORDS
Non-Newtonian Jeffrey's fluid model;
Semi-infinite vertical plate;
Deborah number;
Heat generation;
Thermal radiation;
Retardation time

Abstract The nonlinear, steady state boundary layer flow, heat and mass transfer of an incompressible non-Newtonian Jeffrey's fluid past a semi-infinite vertical plate is examined in this article. The transformed conservation equations are solved numerically subject to physically appropriate boundary conditions using a versatile, implicit finite-difference Keller box technique. The influence of a number of emerging non-dimensional parameters, namely Deborah number (De), ratio of relaxation to retardation times (λ), Buoyancy ratio parameter (N), suction/injection parameter (f_w), Radiation parameter (F), Prandtl number (Pr), Schmidt number (Sc), heat generation/absorption parameter (Δ) and dimensionless tangential coordinate (ξ) on velocity, temperature and concentration evolution in the boundary layer regime is examined in detail. Also, the effects of these parameters on *surface heat transfer rate, mass transfer rate* and *local skin friction* are investigated. This model finds applications in metallurgical materials processing, chemical engineering flow control, etc.

1. Introduction

Non-Newtonian transport phenomena arise in many branches of process mechanical, chemical and materials engineering. Such fluids exhibit shear-stress-strain relationships which diverge significantly from the classical Newtonian (Navier-Stokes) model. Most non-Newtonian models involve some form of modification to the momentum conservation equations. These include power-law fluids [1], viscoelastic fluid model [2], Walters-B short memory models [3], Oldroyd-B models [4], differential Reiner-Rivlin models [5,6], Bingham plastics [7], tangent hyperbolic models [8], Eyring-Powell

* Corresponding author.
E-mail addresses: abdulsgaffar0905@gmail.com (S. Abdul Gaffar), rcpmaths@gmail.com (V. Ramachandra Prasad), eddulakr@gmail.com (E. Keshava Reddy).
Peer review under responsibility of Ain Shams University.
Production and hosting by Elsevier

http://dx.doi.org/10.1016/j.asej.2016.09.003
2090-4479 © 2016 Ain Shams University. Production and hosting by Elsevier B.V.

Nomenclature

C	concentration
C_f	skin friction coefficient
c_p	specific heat parameter
De	Deborah number
D_m	mass (species) diffusivity
f	non-dimensional steam function
F	thermal radiation
$\mathbf{g}$	acceleration due to gravity
Gr	Grashof number
K	thermal diffusivity
k	thermal conductivity
k^*	mean absorption coefficient
L	characteristic length
m	pressure gradient parameter
Nu	heat transfer rate (local Nusselt number)
Pr	Prandtl number
q_r	radiative heat flux
$\mathbf{S}$	Cauchy stress tensor
Sc	local Schmidt number
Sh	mass transfer rate (Sherwood number)
T	temperature of the fluid
u, v	non-dimensional velocity components along the x- and y-directions, respectively
x	streamwise coordinate
y	transverse coordinate
Greek symbols	
α	thermal diffusivity
β	coefficient of thermal expansion
β^*	coefficient of concentration expansion
λ	ratio of relaxation to retardation times
λ_1	retardation time
η	dimensionless radial coordinate
μ	dynamic viscosity
ν	kinematic viscosity
θ	non-dimensional temperature
ϕ	non-dimensional concentration
ρ	density of fluid
ξ	dimensionless tangential coordinate
ψ	dimensionless stream function
Δ	heat generation (source)/heat absorption (sink) parameter
σ^*	Stefan-Boltzmann constant
Subscripts	
w	surface conditions
∞	free stream conditions

models [9], nano non-Newtonian fluid models [59] and Maxwell models [10].

Among the several non-Newtonian models proposed, Jeffrey's fluid model is significant because Newtonian fluid model can be deduced from this as a special case by taking $\lambda_1 = 0$. Further, it is speculated that the physiological fluids such as blood exhibit Newtonian and non-Newtonian behaviors during circulation in a living body. As with a number of rheological models developed, the Jeffrey's model has proved quite successful. This simple, yet elegant rheological model was introduced originally to simulate earth crustal flow problems [11]. This model [12] constitutes a viscoelastic fluid model which exhibits shear thinning characteristics, yield stress and high shear viscosity. The Jeffrey's fluid model degenerates to a Newtonian fluid at a very high wall shear stress i.e. when the *wall stress is much greater than yield stress*. This fluid model also approximates reasonably well the rheological behavior of other liquids including physiological suspensions, foams, geological materials, cosmetics, and syrups. Interesting studies employing this model include peristaltic transport of Jeffery fluid under the effect of magnetohydrodynamic [13], peristaltic flow of Jeffery fluid with variable-viscosity [14], Radiative flow of Jeffery fluid in a porous medium with power law heat flux and heat source [15]. Vajravelu et al. [16] presented the influence of free convection on nonlinear peristaltic transport of Jeffrey fluid in a finite vertical porous stratum using the Brinkman model. Lakshminarayana et al. [17] discussed the influence of slip and heat transfer on the peristatic transport of Jeffrey fluid in a vertical asymmetric channel in porous medium. The governing equations are solved using perturbation technique. The peristaltic flow of a conducting Jeffrey fluid in an inclined asymmetric channel was investigated by K. Vajravelu et al. [18] using perturbation technique. Vajravelu et al. [19] reported the peristaltic flow of Jeffrey fluid in a vertical porous stratum with heat transfer under long wavelength and low Reynolds number assumptions.

The heat transfer analysis of boundary layer flow with radiation is important in various material processing operations including high temperature plasmas, glass fabrication, and liquid metal fluids. When coupled with thermal convection flows, these transport phenomena problems are highly nonlinear. At a high temperature the presence of thermal radiation changes the distribution of temperature in the boundary layer, which in turn affects the heat transfer at the wall. A number of studies have appeared that consider multi-physical radiative-convective flows. Recently, Nadeem et al. [20] reported the magnetic field effects on boundary layer flow of Eyring-Powell fluid from a stretching sheet. Noor et al. [21] used the Rosseland model to study radiation effects on hydromagnetic convection with thermophoresis along an inclined plate. Further, studies employing the Rosseland model include Gupta et al. [22] who examined on radiative convective micropolar shrinking sheet flow, Cortell [23] who investigated non-Newtonian dissipative radiative flow, and Bargava et al. [24] who studied radiative-convection micropolar flow in porous media. Akbar et al. [25] reported the dual solutions in MHD stagnation-point flow of a Prandtl fluid past a shrinking sheet by shooting method.

Convective boundary-layer flows are often controlled by injecting or withdrawing fluid through a heat surface. This can lead to enhanced heating or cooling of the system and can help to delay the transition from laminar to turbulent flow.

Free convection flow of pure fluids past a semi-infinite vertical plate, at normal temperature, was first presented by Pohlhausen [26], who obtained a solution by the momentum integral method. A similarity solution for this problem was solved, for the first time, by Ostrach [27]. The application of free convection flows, which occur in nature and in engineering processes, is very wide and has been extensively, considered by Jaluria [28]. The simplest physical model of such flow is the two-dimensional laminar flow along a vertical flat plate. Extensive studies have been conducted on this type of flow by several authors [29–32]. Application of this model can be found in the area of reactor safety, combustion flames and solar collectors, as well as building energy conservation [33]. Takhar et al. [34] studied the combined convection-radiation interaction along a vertical flat plate in a porous medium.

The case of uniform suction and blowing through an isothermal vertical wall was treated first by Sparrow and Cess [35]; they obtained a series solution which is valid near the leading edge. This problem was considered in more detail by Merkin [36], who obtained asymptotic solutions, valid at large distances from the leading edge, for both the suction and blowing. Using the method of matched asymptotic expansion, the next order corrections to the boundary-layer solutions for this problem were obtained by Clarke [37], who extended the range of applicability of the analyses by not invoking the usual Boussinesq approximation. The effect of strong suction and blowing from general body shapes which admit a similarity solution has been given by Merkin [38]. A transformation of the equations for general blowing and wall temperature variations has been given by Vedhanayagam et al. [39]. The case of a heated isothermal horizontal surface with transpiration has been discussed in some detail first by Clarke and riley [40]. Free convection on a horizontal plate with blowing and suction was studied by Lin and Yu [41]. Chamkha et al. [42–44] conducted a theoretical study of suction and injection in free and mixed convection heat and mass transfer over different geometries, viz. plate, stretching cylinder, and stretching surface. Hossain et al. [45] studied the effect of radiation on free convection flow with variable viscosity from a porous vertical plate. The free convective heat and mass transfer flow is a comparatively recent development in the field of fluid mechanics and the different mathematical models and correlations which have been developed can be applied to many industrial applications, such as chemical or drying processes.

The current work presents a numerical study of non-similar free convection boundary layer flow, heat and mass transfer of Jeffrey's non-Newtonian fluid past a semi-infinite vertical plate with thermal radiation and heat generation/absorption. The non-dimensional equations with associated dimensionless boundary conditions constitute a highly nonlinear, coupled two-point boundary value problem. Keller's implicit finite difference "box" scheme is implemented to solve the problem. The effects of the emerging thermophysical parameters, namely *Deborah number* (De)*, ratio of relaxation to retardation times* (λ)*, thermal radiation parameter* (F)*, suction/injection parameter* (f_w) *and heat generation/absorption parameter* (Δ) on the velocity, temperature, concentration, local skin friction, heat transfer rate and mass transfer rate characteristics are studied. The present problem has to the authors' knowledge not appeared thus far in the scientific literature and is relevant to polymeric manufacturing processes and nuclear waste simulations.

2. Mathematical model

A steady, laminar, two-dimensional, incompressible, viscous, buoyancy-driven free convection flow, heat and mass transfer past a semi-infinite vertical plate to Jeffrey's fluid in the presence of heat source/sink, suction/injection and thermal radiation is studied, as illustrated in Fig. 1. The x-coordinate (tangential) is measured along the vertical plate in the upward direction and y-coordinate (radial) is measured normal to the plate. The corresponding velocities in x and y directions are u and v respectively. The gravitational acceleration $\boldsymbol{g}$, acts vertically downwards. The flow is driven by buoyancy effects, which are generated by the gradients in temperature and concentration field of a dissolved species. Magnetic Reynolds number is assumed to be small enough to neglect magnetic induction effects. Hall current and ionslip effects are also neglected since the magnetic field is weak. We also assume that the Boussinesq approximation holds i.e. the density variation is only experienced in the buoyancy term in the momentum equation.

Both the semi-infinite vertical plate and Jeffrey's fluid are maintained initially at a constant temperature and concentration. Instantaneously, they are raised to a temperature $T_w(>T_\infty)$ and concentration $C_w(>C_\infty)$, where the latter (ambient) temperature and concentration of the fluid are sustained constant. The Cauchy stress tensor, $\boldsymbol{S}$, of a Jeffrey's non-Newtonian fluid [46] takes the form as follows:

$$\boldsymbol{T} = -p\boldsymbol{I} + \boldsymbol{S}, \boldsymbol{S} = \frac{\mu}{1+\lambda}(\dot{\gamma} + \lambda_1\ddot{\gamma}) \tag{1}$$

where dot above a quantity denotes the material time derivative and $\dot{\gamma}$ is the shear rate. The Jeffrey's model provides an elegant formulation for simulating retardation and relaxation effects arising in non-Newtonian polymer flows. The shear rate and gradient of shear rate are further defined in terms of velocity vector, $\boldsymbol{V}$, as follows:

$$\dot{\gamma} = \nabla V + (\nabla V)^T \tag{2}$$

$$\ddot{\gamma} = \frac{d}{dt}(\dot{\gamma}) \tag{3}$$

Introducing the boundary layer approximations, and incorporating the stress tensor for a Jeffrey's fluid in the momentum equation (in differential form), the conservation equations take the following form:

$$\frac{\partial u}{\partial x} + \frac{\partial v}{\partial y} = 0 \tag{4}$$

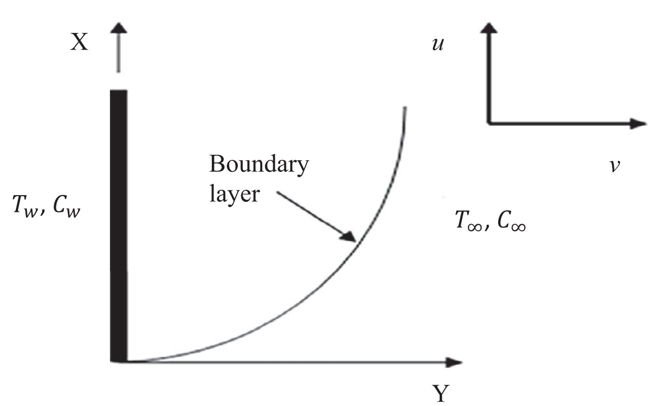

Figure 1 Flow configuration and coordinate system.

$$u\frac{\partial u}{\partial x}+v\frac{\partial u}{\partial y}=\frac{v}{1+\lambda}\left(\frac{\partial^2 u}{\partial y^2}+\lambda_1\left(u\frac{\partial^3 u}{\partial x\partial y^2}-\frac{\partial u}{\partial x}\frac{\partial^2 u}{\partial y^2}+\frac{\partial u}{\partial y}\frac{\partial^2 u}{\partial x\partial y}+v\frac{\partial^3 u}{\partial y^3}\right)\right)+g\beta(T-T_\infty)+g\beta^*(C-C_\infty) \quad (5)$$

$$u\frac{\partial T}{\partial x}+v\frac{\partial T}{\partial y}=\alpha\frac{\partial^2 T}{\partial y^2}-\frac{1}{\rho c_p}\frac{\partial q_r}{\partial y}+\frac{Q_0}{\rho c_p}(T-T_\infty) \quad (6)$$

$$u\frac{\partial C}{\partial x}+v\frac{\partial C}{\partial y}=D_m\frac{\partial^2 C}{\partial y^2} \quad (7)$$

The appropriate boundary conditions are as follows:

$$\begin{array}{llllll} At & y=0, & u=0, & v=V_w(x), & T=T_w, & C=C_w \\ As & y\to\infty, & u\to 0, & v\to 0, & T\to T_\infty, & C\to C_\infty \end{array} \quad (8)$$

The Jeffrey's fluid model, introduces a number of *mixed* derivatives in the momentum boundary layer equation (5) and in particular two *third order* derivatives $u\frac{\partial^3 u}{\partial x\partial y^2}$ and $v\frac{\partial^3 u}{\partial y^3}$, making the system an order higher than the *classical Navier-Stokes (Newtonian) viscous flow* model. The non-Newtonian effects feature in the shear terms only of Eq. (5) and not the convective (acceleration) terms. The third term on the right hand side of Eq. (5) represents the *thermal buoyancy force* and couples the velocity field with the temperature field equation (6). The fourth term on right hand side of Eq. (5) represents the *species buoyancy effect (mass transfer)* and couples Eq. (5) to the species diffusion equation (7). Viscous dissipation effects are neglected in the model.

In Eq. (6) the penultimate term on the right side is the thermal radiation flux contribution based on Rosseland approximation [47,48]. This formulation allows the transformation of the governing integro-differential equation for radiative energy balance into electrostatic potential (Coulomb's law) which is valid for optically-thick media in which radiation only propagates a limited distance prior to experiencing scattering or absorption. It can be shown that the local intensity is caused by radiation emanating from nearby locations in the vicinity of which the emission and scattering are comparable to the location under consideration. For zones where conditions are appreciably different, the radiation has been shown to be greatly attenuated prior to arriving at the location being analyzed. The energy transfer depends only on the conditions in the area near the position under consideration. In applying the Rosseland assumption, it is assumed that refractive index of the medium is constant, intensity within the porous medium is nearly isotropic and uniform and wavelength regions exist where the optical thickness is greater than 5. Further details are available in Bég et al. [49]. The final term on the right hand side of Eq. (6) is the *heat source/sink contribution*. The Rosseland diffusion flux model is an *algebraic approximation* and defined as follows:

$$q_r=\frac{4\sigma^*}{3k^*}\frac{\partial T^4}{\partial y} \quad (9)$$

where k^*- mean absorption coefficient and σ^*- Stefan–Boltzmann constant. It is customary [47] to express T^4 as a linear function of temperature. Expanding T^4 using Taylor series and neglecting higher order terms leads to the following:

$$T^4\cong 4T_\infty^3 T-3T_\infty^4 \quad (10)$$

Substituting (10) into (9), eventually leads to the following version of the heat conservation equation (6):

$$u\frac{\partial T}{\partial x}+v\frac{\partial T}{\partial y}=\alpha\frac{\partial^2 T}{\partial y^2}+\frac{16\sigma^* T_\infty^3}{3k^*\rho c_p}\frac{\partial^2 T}{\partial y^2}+\frac{Q_0}{\rho c_p}(T-T_\infty) \quad (11)$$

To transform the boundary value problem to a dimensionless one, we introduce a stream function ψ defined by the *Cauchy-Riemann* equations, $u=\frac{\partial\psi}{\partial y}$ and $v=\frac{\partial\psi}{\partial x}$.

The mass conservation Eq. (4) is automatically satisfied.

The following dimensionless variables are introduced into Eqs. (5)–(8):

$$\xi=\left(\frac{x}{L}\right)^{1/2},\quad \eta=C_1 y x^{-1/4},\quad C_1=\left(\frac{g\beta(T_w-T_\infty)}{4v^2}\right),$$
$$\psi=4vC_1x^{3/4}f,\quad \Pr=\frac{v\rho c_p}{k},\quad Sc=\frac{v}{D_m}$$
$$\theta(\xi,\eta)=\frac{T-T_\infty}{T_w-T_\infty},\quad \phi(\xi,\eta)=\frac{C-C_\infty}{C_w-C_\infty},$$
$$Gr=\frac{g\beta(T_w-T_\infty)L^3}{v^2},\quad De=\frac{\lambda_1 vC_1^2}{x^{1/2}} \quad (12)$$

The resulting momentum, energy and concentration boundary layer equations take the following form:

$$\frac{f'''}{1+\lambda}+3ff''-2(f')^2+(\theta+N\varphi)+\frac{De}{1+\lambda}(f''^2-2f'f'''-3ff^{iv})=2\xi\left(f'\frac{\partial f'}{\partial\xi}-f''\frac{\partial f}{\partial\xi}-\frac{De}{1+\lambda}\left(f'\frac{\partial f'''}{\partial\xi}-f'''\frac{\partial f'}{\partial\xi}+f''\frac{\partial f''}{\partial\xi}-f^{iv}\frac{\partial f}{\partial\xi}\right)\right) \quad (13)$$

$$\frac{\theta''}{Pr}\left(1+\frac{4}{3F}\right)+3f\theta'+\Delta\theta=2\xi\left(f'\frac{\partial\theta}{\partial\xi}-\theta'\frac{\partial f}{\partial\xi}\right) \quad (14)$$

$$\frac{\phi''}{Sc}+3f\phi'=2\xi\left(f'\frac{\partial\phi}{\partial\xi}-\phi'\frac{\partial f}{\partial\xi}\right) \quad (15)$$

The corresponding non-dimensional boundary conditions for the collectively eighth order, multi-degree partial differential equation system defined by Eqs. (13)–(15) assume the following form:

$$\begin{array}{llllll} At & \eta=0, & f=f_w, & f'=0, & \theta=1, & \phi=1 \\ As & \eta\to\infty, & f'\to 0, & f''\to 0, & \theta\to 0, & \phi\to 0 \end{array} \quad (16)$$

Here primes denote the differentiation with respect to η. $N=\frac{\beta^*(C_w-C_\infty)}{\beta(T_w-T_\infty)}$ is the concentration to thermal buoyancy ratio parameter, $F=\frac{Kk^*}{4\sigma^* T_\infty^3}$ is the radiation parameter, and $\Delta=\frac{Q_0 x^2}{\rho v c_p Re_x}$ is the dimensionless heat generation/absorption coefficient. $f_w=\frac{V_w x^{1/4}}{3vC_1}$ is the suction/blowing parameter. $f_w<0$ for $V_w>0$ is the case of blowing and $f_w>0$ for $V_w<0$ is the case of suction. The $f_w=0$ is the special case of a solid plate surface. The chemical engineering design quantities of physical interest including the skin-friction coefficient (shear stress), Nusselt number (heat transfer rate) and Sherwood number (mass transfer rate) can be defined using the transformations described above with the following expressions:

$$C_f = 4\nu\mu C_1^3 x^{1/4} f''(\xi, 0) \tag{17}$$

$$Nu = -k\Delta T C_1 x^{-1/4}\theta'(\xi, 0) \tag{18}$$

$$Sh = -D\Delta C\, C_1 x^{-1/4}\phi'(\xi, 0) \tag{19}$$

The location, $\xi \sim 0$, corresponds to the vicinity of the *lower stagnation point* on the wedge. For this scenario, the model defined by Eqs. (13)–(15) contracts to an *ordinary* differential boundary value problem:

$$\frac{f'''}{1+\lambda} + 3ff'' - 2(f')^2 + (\theta + N\varphi) + \frac{De}{1+\lambda}(-2f'f''' + f''^2 - 3ff^{iv}) = 0 \tag{20}$$

$$\frac{\theta''}{Pr}\left(1 + \frac{4}{3F}\right) + 3f\theta' + \Delta\theta = 0 \tag{21}$$

$$\frac{\phi''}{Sc} + 3f\phi' = 0 \tag{22}$$

3. Finite difference solutions

The Keller-Box implicit difference method is utilized to solve the nonlinear boundary value problem defined by Eqs. (13)–(15) with boundary conditions (16). This technique, despite recent developments in other numerical methods, remains a powerful and very accurate approach for boundary layer flow equation systems *which are generally parabolic in nature*. It is unconditionally stable and achieves exceptional accuracy. An excellent summary of this technique is given in Keller [50]. Magnetohydrodynamic applications of Keller's method are reviewed in Bég [51]. This method has also been applied successfully in many rheological flow problems in recent years. These include oblique micropolar stagnation flows [52], Walter's B viscoelastic flows [53], Stokesian couple stress flows [54], hyperbolic-tangent convection flows from curved bodies [55], micropolar nanofluids [56], magnetic Williamson fluids [57] and Maxwell fluids [58]. The Keller-Box discretization is *fully coupled* at each step which reflects the physics of parabolic systems – which are also fully coupled. Discrete calculus associated with the Keller-Box scheme has also been shown to be fundamentally different from all other mimetic (physics capturing) numerical methods, as elaborated by Keller [50]. The Keller Box Scheme comprises four stages:

(1) Reduction of the Nth order partial differential equation system to N first order equations.
(2) Finite difference discretization.
(3) Quasilinearization of non-linear Keller Algebraic Equations.
(4) Block-tridiagonal elimination of linear Keller Algebraic Equations.

4. Results and discussion

Comprehensive results are obtained and are presented in Figs. 2–10. The numerical problem comprises of two independent variables (ξ,η), three dependent fluid dynamic variables (f, θ,ϕ) and eight thermo-physical and body force control parameters, namely, De, λ, Δ, F, N, Pr, Sc, f_w. The following default parameter values i.e. De = 0.1, λ = 0.2, Δ = 0.1, f_w = 1.0, F = 0.5, N = 0.5, Pr = 0.71, Sc = 0.6 are prescribed (unless otherwise stated).

In Figs. 2a–2c, we depict the evolution of velocity (f'), temperature (θ) and concentration (ϕ) functions with a variation in De. Dimensionless velocity (Fig. 2a) is considerably decreased with increasing De. De clearly arises in connection with high order derivatives in Eq. (13) i.e. $\frac{De}{1+\lambda}(-2f'f''' + f''^2 - 3ff^{iv})$ and $\xi\left(-\frac{De}{1+\lambda}\left[f'\frac{\partial f'''}{\partial\xi} - f'''\frac{\partial f'}{\partial\xi} + f''\frac{\partial f''}{\partial\xi} - f^{iv}\frac{\partial f}{\partial\xi}\right]\right)$. In Fig. 2b, an increase in De is seen to considerably increase temperatures throughout the boundary layer regime. Although De does not arise in the thermal boundary layer equation (14), there is a strong coupling of this equation with the momentum field via the convective terms $\xi\left[f'\frac{\partial\theta}{\partial\xi}\right]$ and $\xi\left[-\theta'\frac{\partial f}{\partial\xi}\right]$. Furthermore, the thermal buoyancy force term, $+\theta$ in the momentum equation (13) strongly couples the momentum flow field to the temperature field. Thermal boundary layer thickness is also elevated with increasing De. Fig. 2c shows a slight increase in concentration is achieved with increasing De values.

Figs. 3a–3c illustrate the effect of λ on the velocity (f'), temperature (θ) and concentration (ϕ) distributions through the boundary layer regime. Velocity is significantly increased with increasing λ. The polymer flow is therefore considerably *accelerated* with an increase in relaxation time (or decrease in retardation time). Conversely, temperature and concentration are depressed slightly with increasing λ. The mathematical model reduces to the *Newtonian viscous flow model* as $\lambda \to 0$ and $De \to 0$, since this negates relaxation, retardation and elasticity effects. The momentum boundary layer equation in this case contracts to the familiar equation for *Newtonian*:

$$f''' + 3ff'' - 2f'^2 + (\theta + N\phi) = 2\xi\left(f'\frac{\partial f'}{\partial\xi} - f''\frac{\partial f}{\partial\xi}\right) \tag{23}$$

The thermal boundary layer equation and concentration Eqs. (14) and (15) remain unchanged.

Figs. 4a–4c present typical profiles for velocity (f'), temperature (θ) and concentration (ϕ) for various values of F. Increasing F, strongly decelerates the flow i.e. decreases velocity. This parameter features in the term, $\frac{1}{\mathrm{Pr}}\left(1 + \frac{4}{3F}\right)\theta''$ in the energy conservation Eq. (14). F represents the relative contribution of *thermal conduction* to *thermal radiation* heat transfer. For F = 1 both modes of heat transfer have the same contribution. Temperatures are therefore also decreased, as observed in Fig. 4b. Conversely, there is a slight enhancement in concentration values with increasing F values, as shown in Fig. 4c.

Figs. 5a–5c present typical profiles for velocity (f'), temperature (θ) and concentration (ϕ) for various values of Δ. Increasing heat generation ($\Delta > 0$) significantly accelerates the flow and also increases temperature magnitudes but reduces concentration values. Conversely, with a heat sink present, ($\Delta < 0$) the flow is retarded (momentum boundary layer thickness is lowered), thermal boundary layer thickness is reduced whereas, concentration boundary layer thickness increases.

Figs. 6a–6c depict the profiles for velocity (f'), temperature (θ) and concentration (ϕ) for various values of buoyancy ratio parameter N. With $N > 0$ the flow is evidently accelerated (Fig. 6a) for some distance from the plate surface. Initially for $N < 0$ i.e. the buoyancy opposed case where thermal and species buoyancy forces act against each other, the flow is

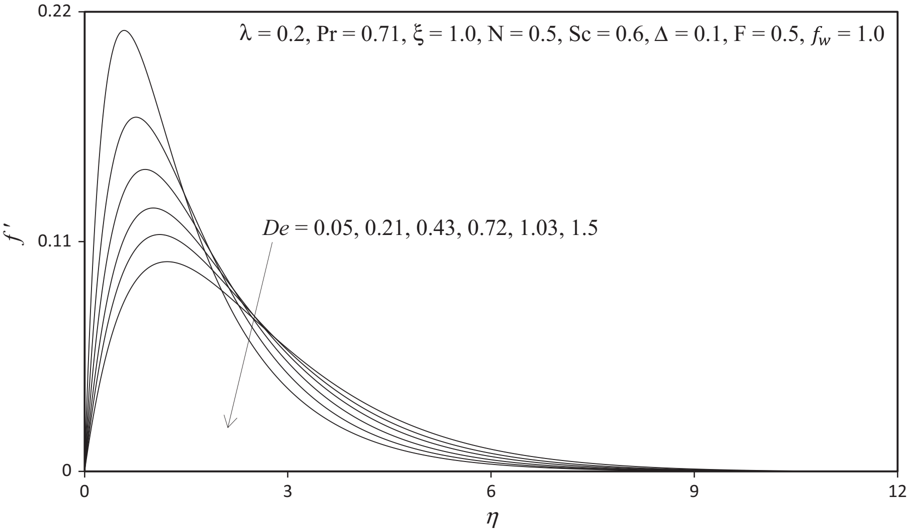

Figure 2a Influence of *De* on velocity profiles.

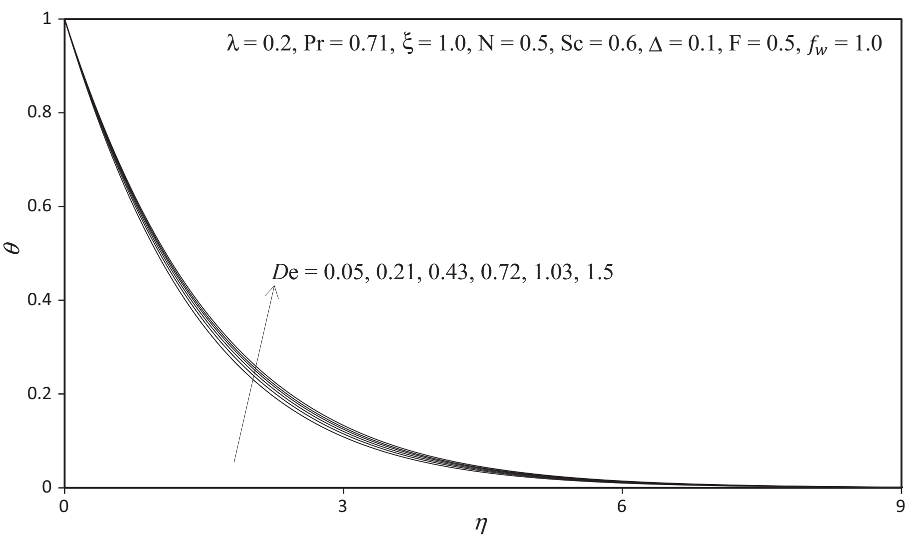

Figure 2b Influence of *De* on temperature profiles.

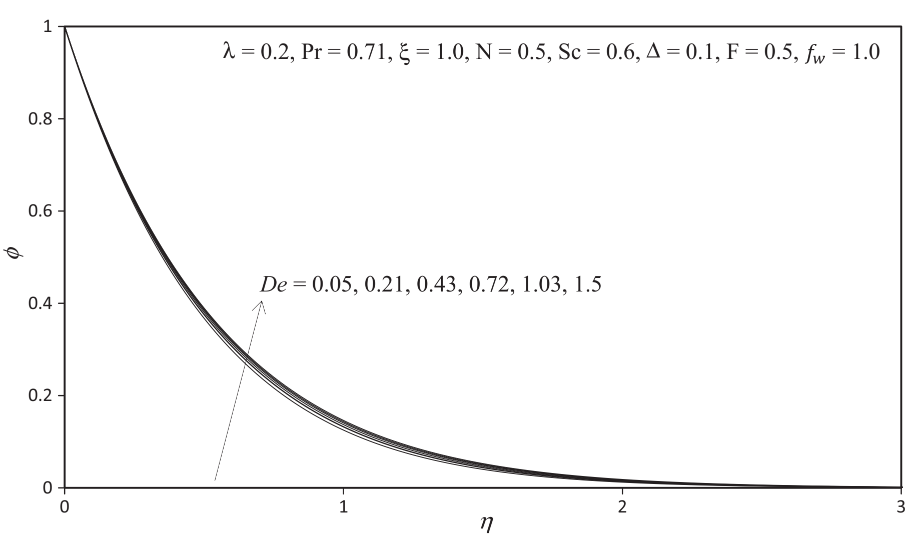

Figure 2c Influence of *De* on concentration profiles.

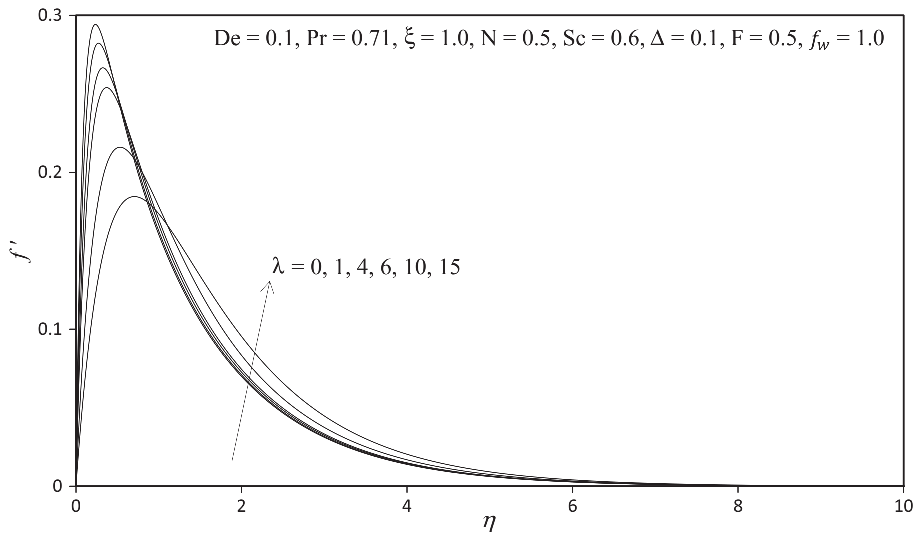

Figure 3a Influence of λ on velocity profiles.

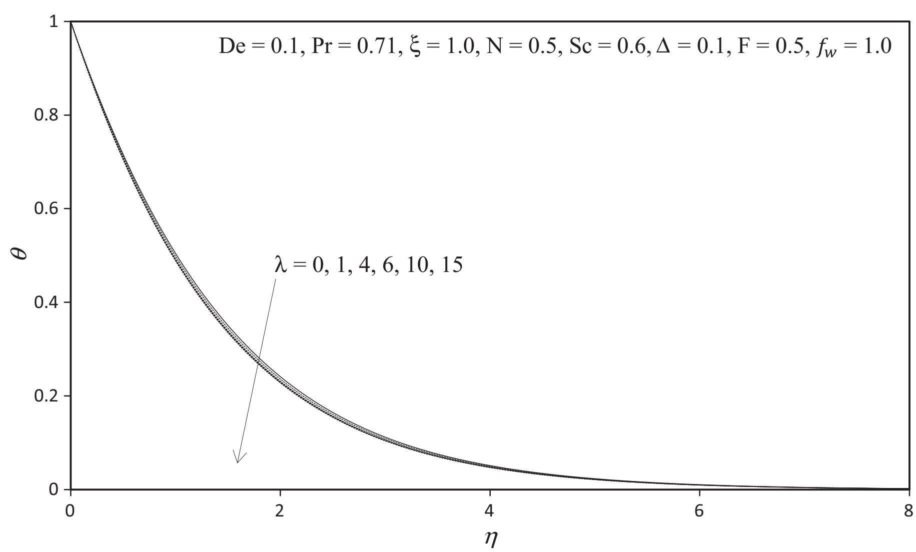

Figure 3b Influence of λ on temperature profiles.

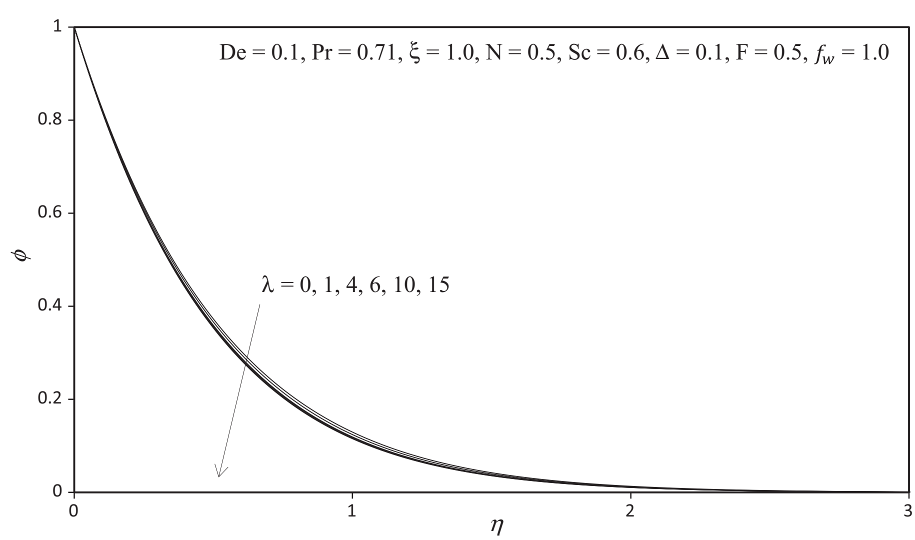

Figure 3c Influence of λ on concentration profiles.

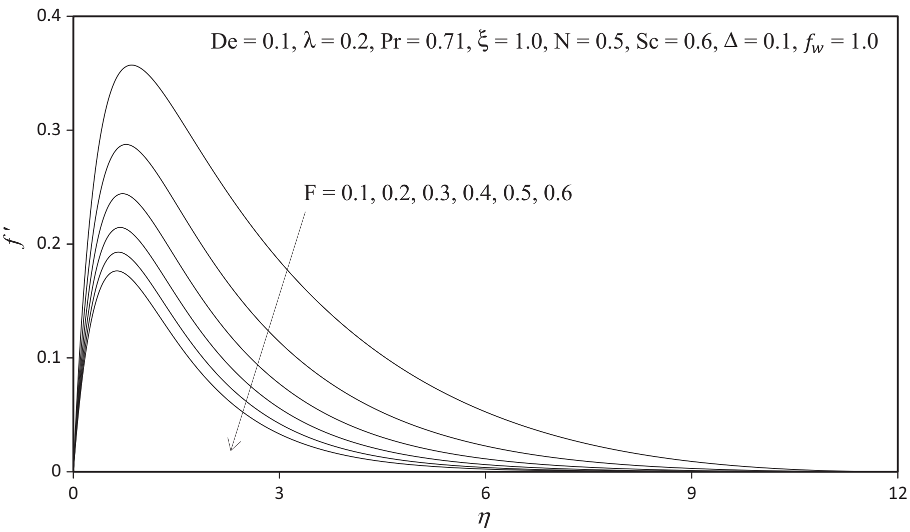

Figure 4a Influence of F on velocity profiles.

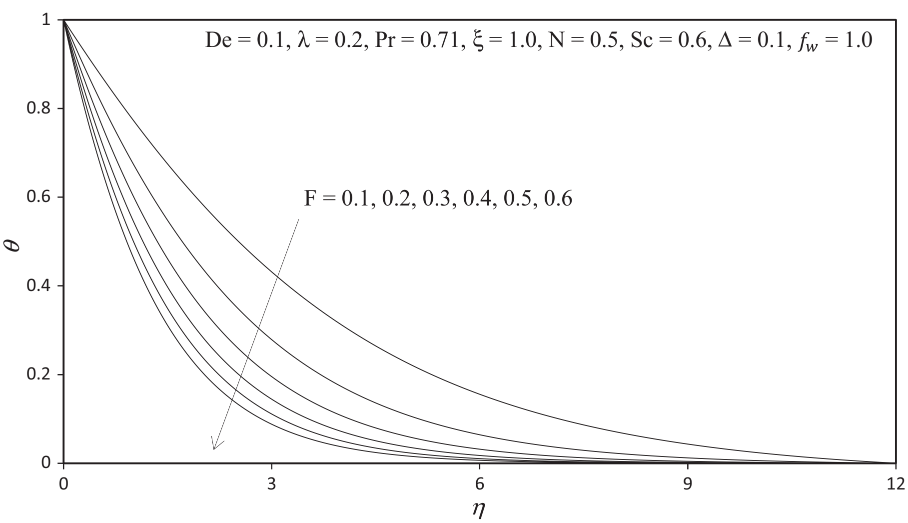

Figure 4b Influence of F on temperature profiles.

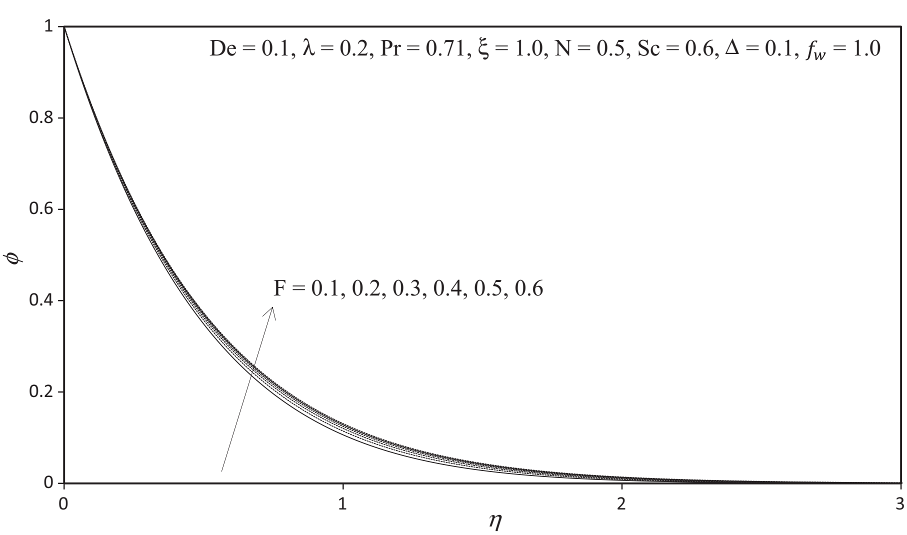

Figure 4c Influence of F on concentration profiles.

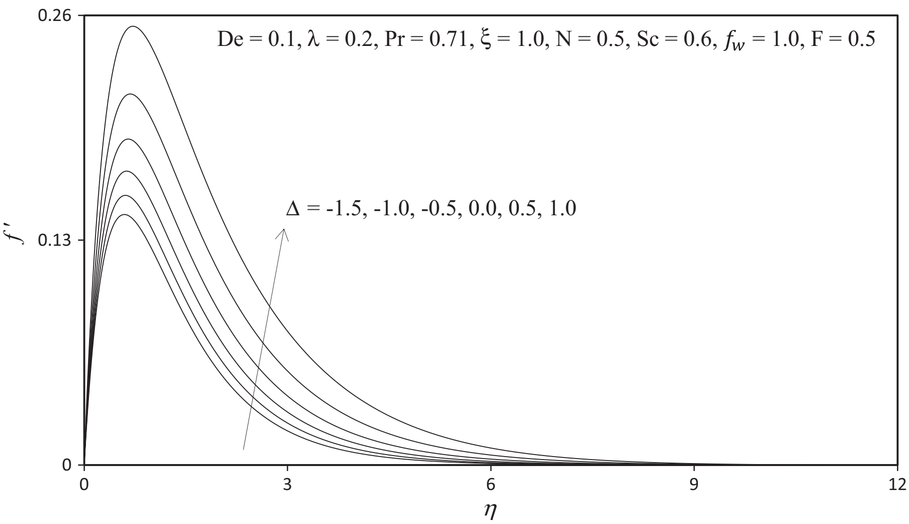

Figure 5a Influence of *Δ* on velocity profiles.

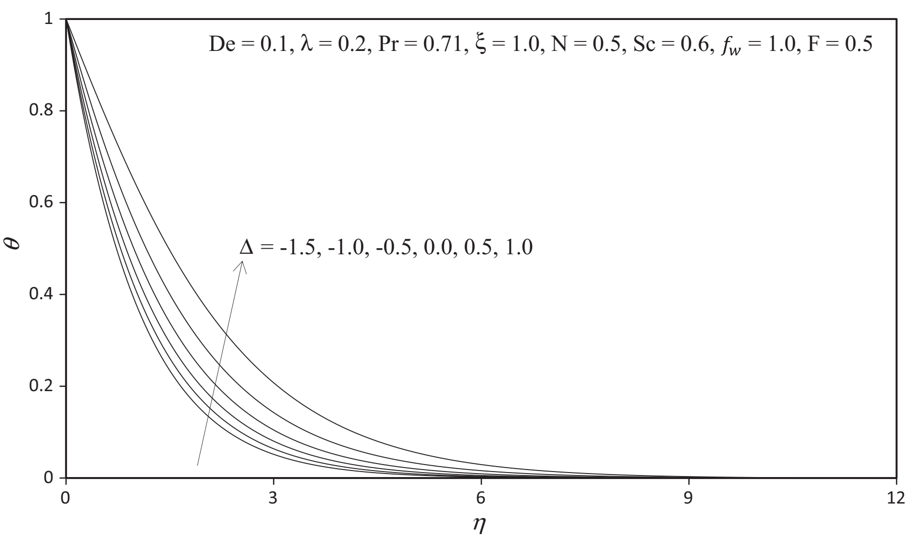

Figure 5b Influence of *Δ* on temperature profiles.

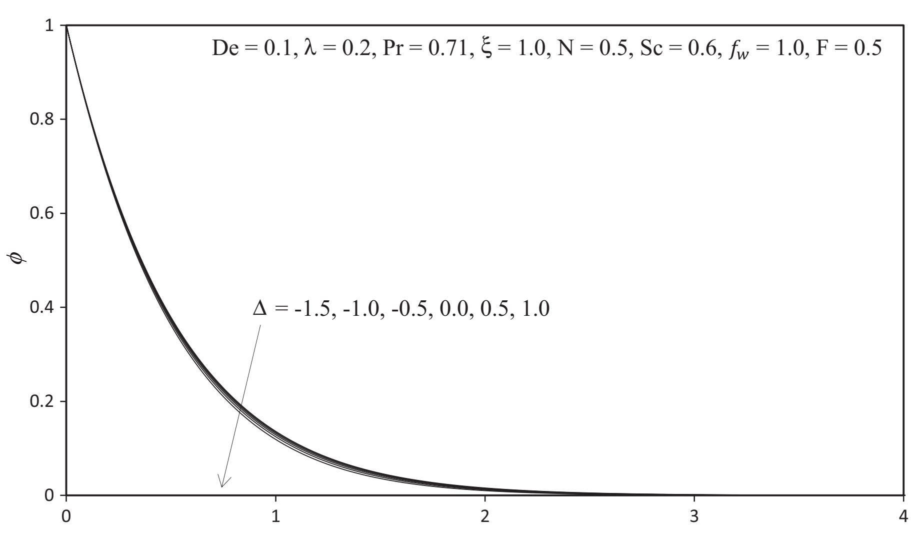

Figure 5c Influence of *Δ* on concentration profiles.

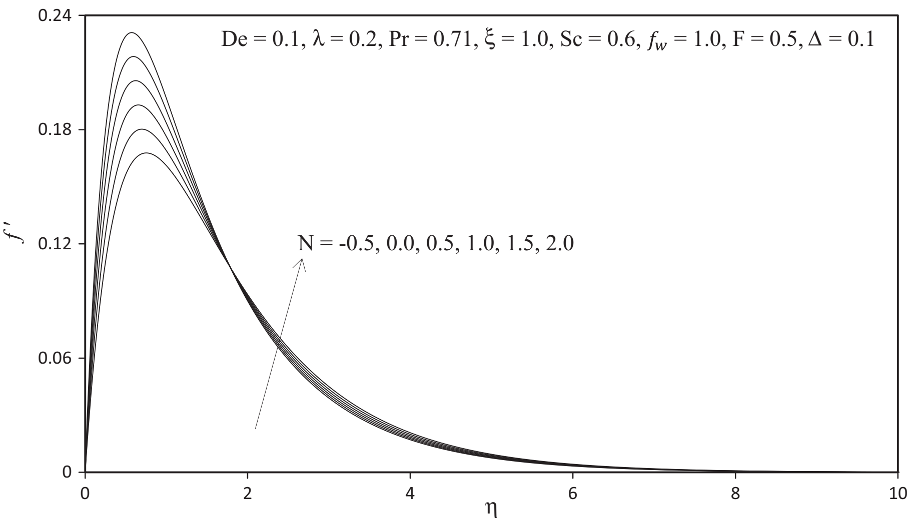

Figure 6a Influence of N on velocity profiles.

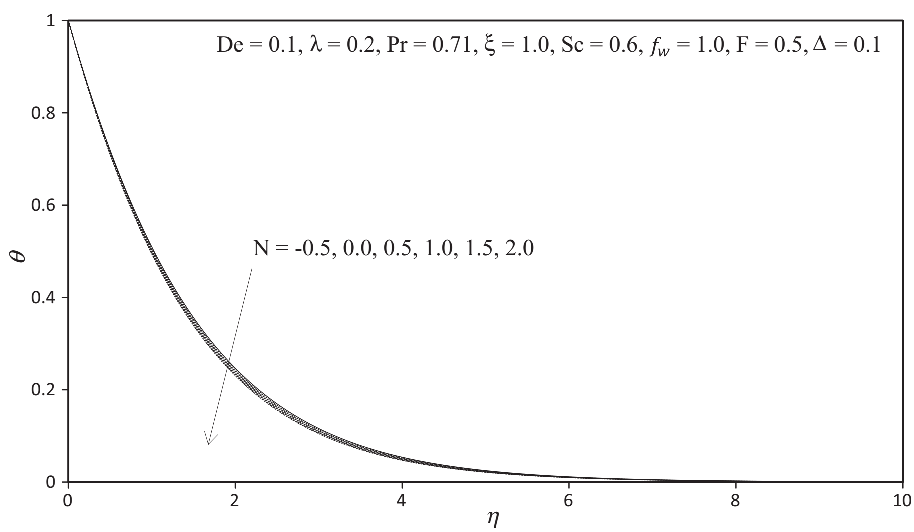

Figure 6b Influence of N on temperature profiles.

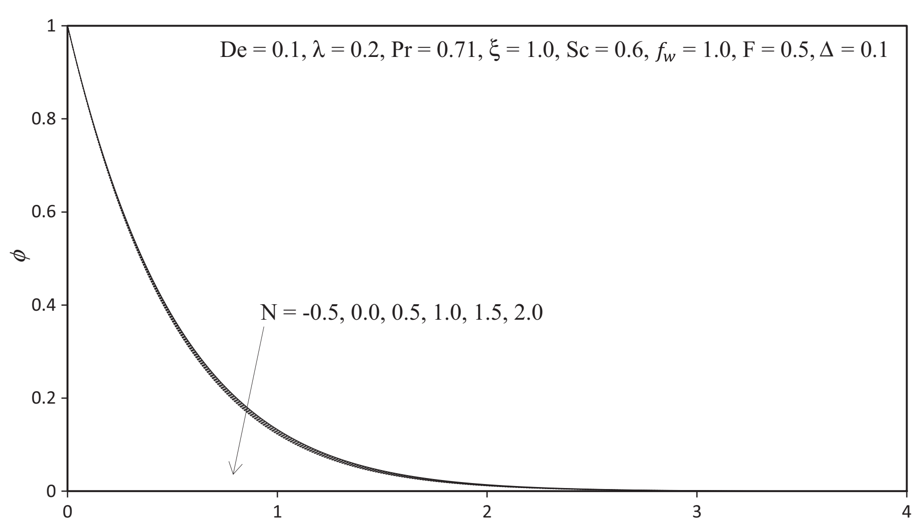

Figure 6c Influence of N on concentration profiles.

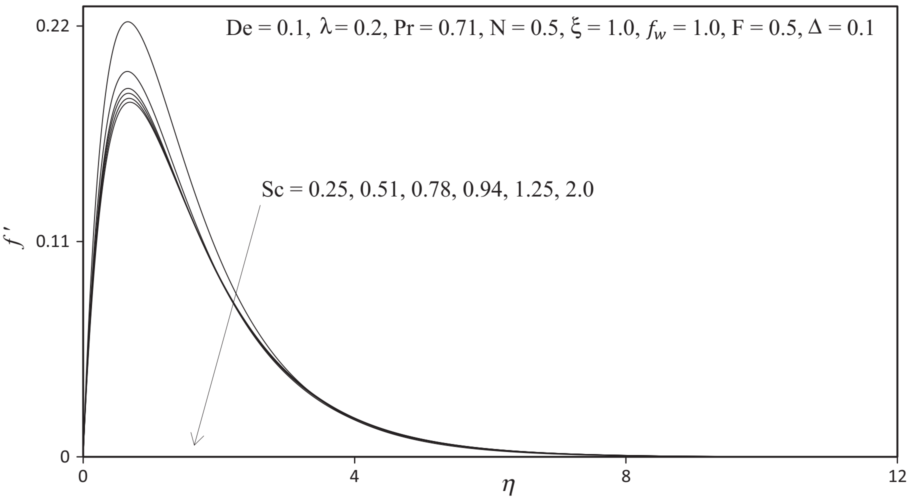

Figure 7a Influence of *Sc* on velocity profiles.

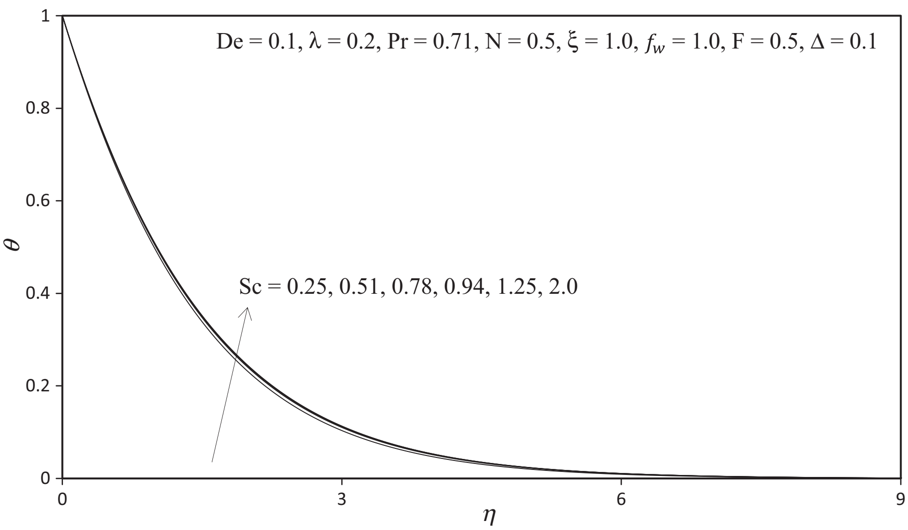

Figure 7b Influence of *Sc* on temperature profiles.

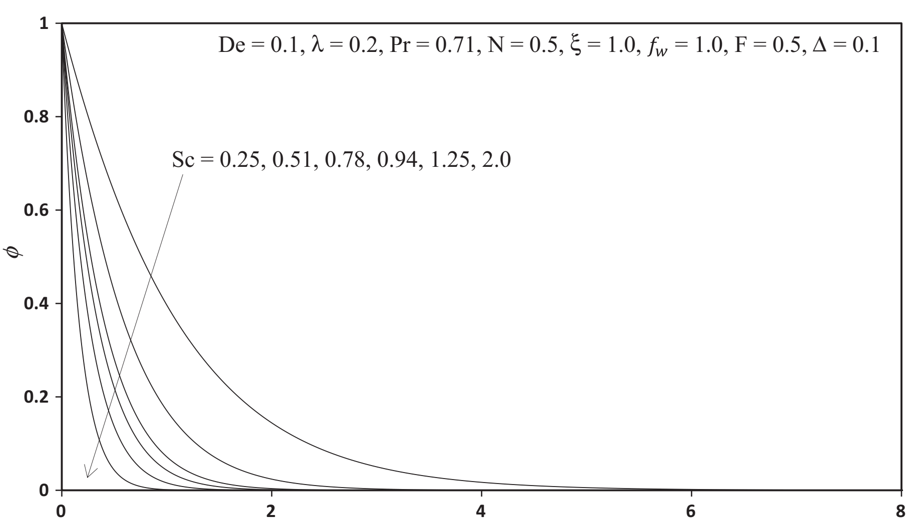

Figure 7c Influence of *Sc* on concentration profiles.

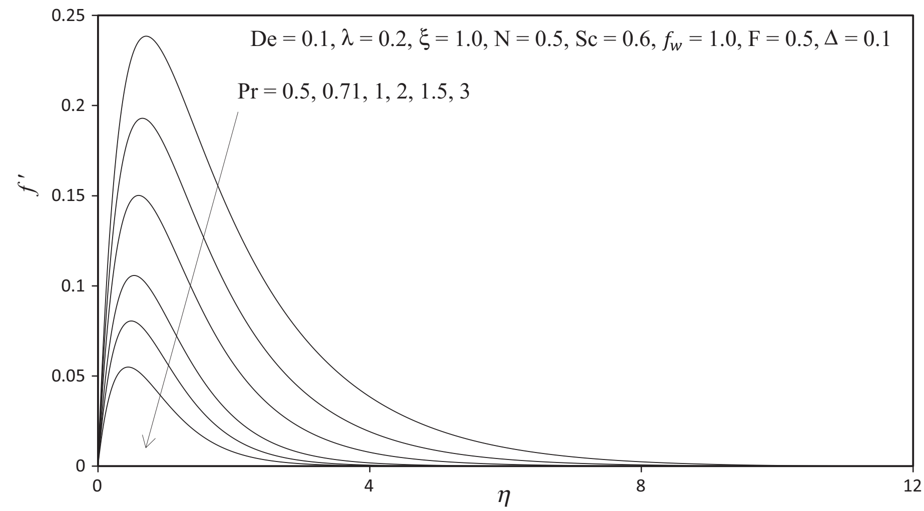

Figure 8a Influence of *Pr* on velocity profiles.

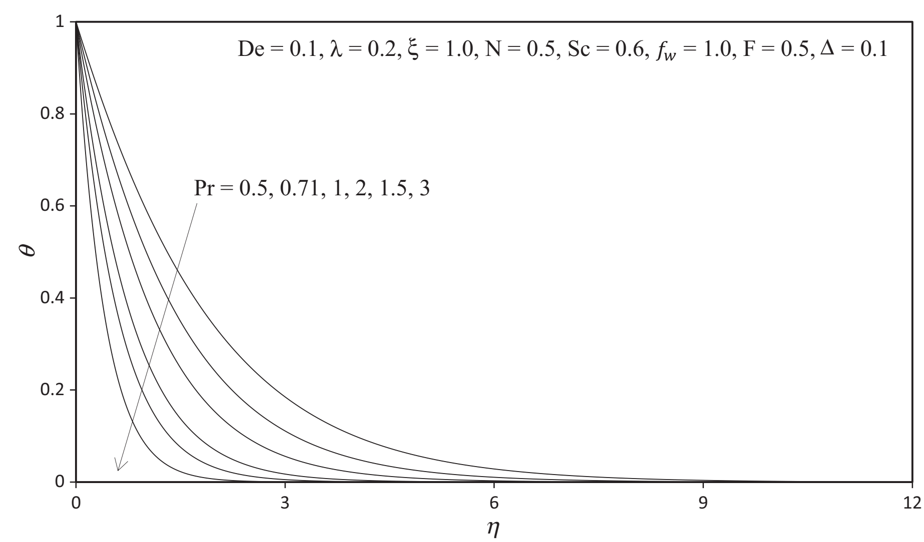

Figure 8b Influence of *Pr* on temperature profiles.

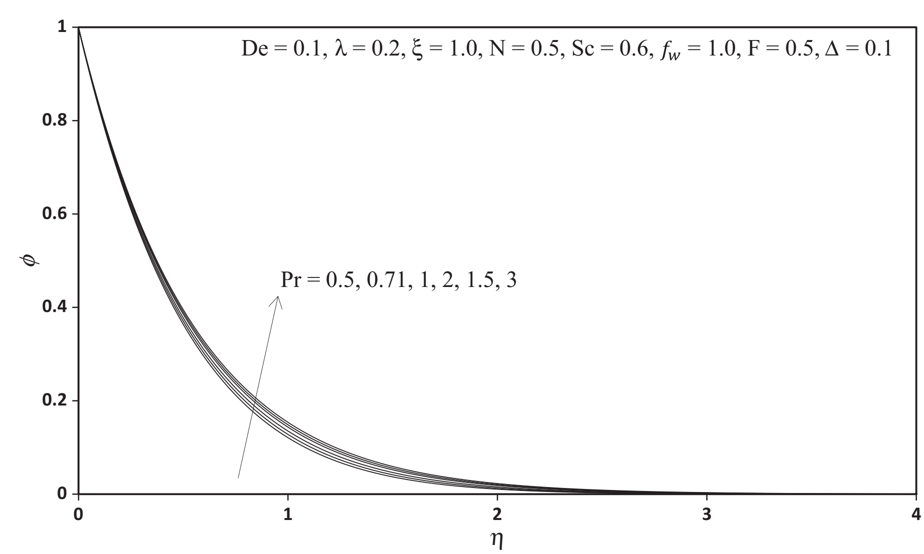

Figure 8c Influence of *Pr* on concentration profiles.

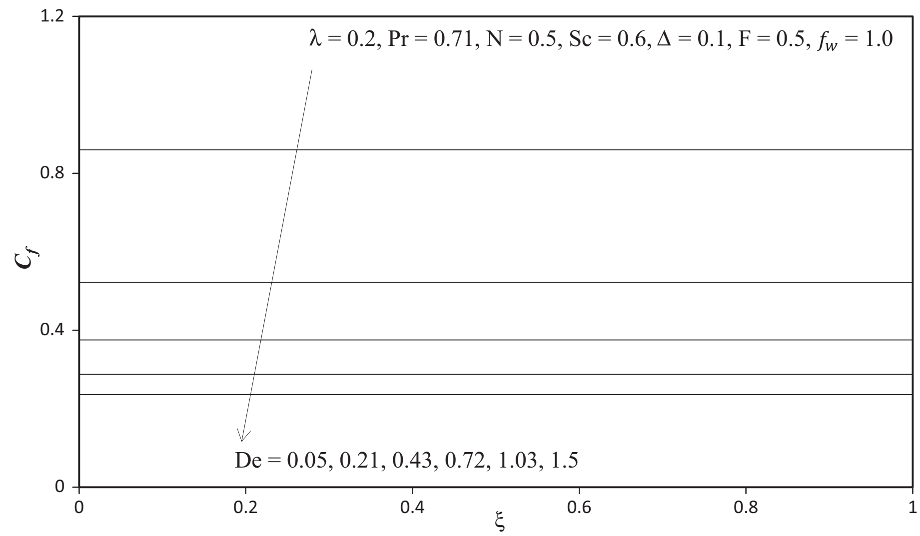

Figure 9a Influence of *De* on local skin friction.

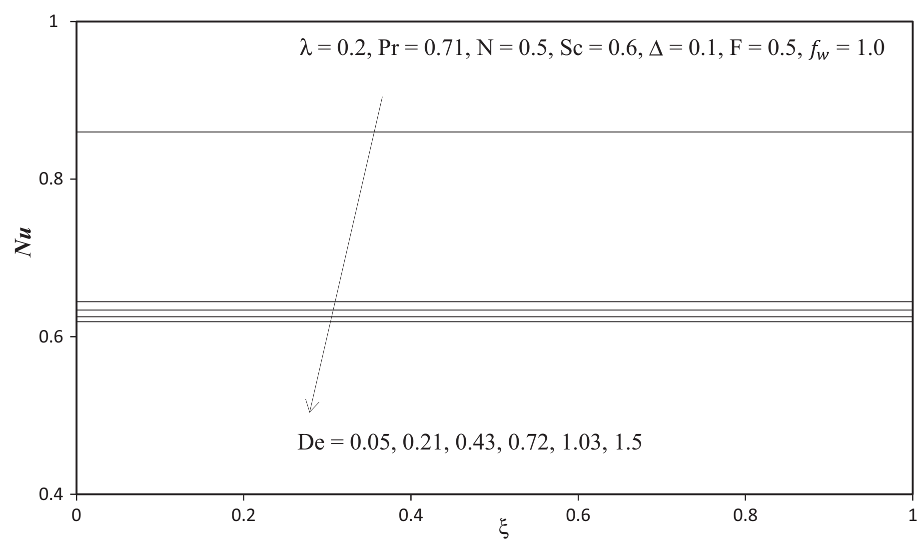

Figure 9b Influence of *De* on Nusselt number.

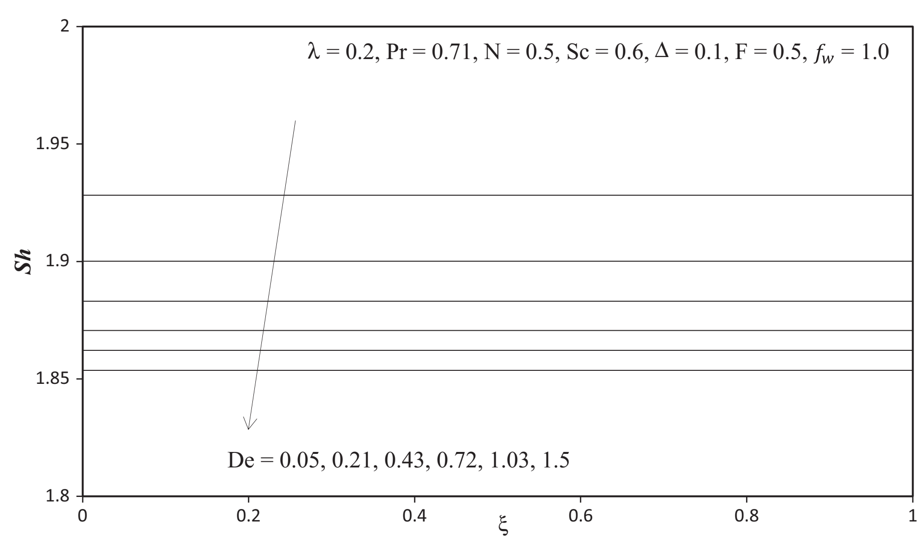

Figure 9c Influence of *De* on Sherwood number.

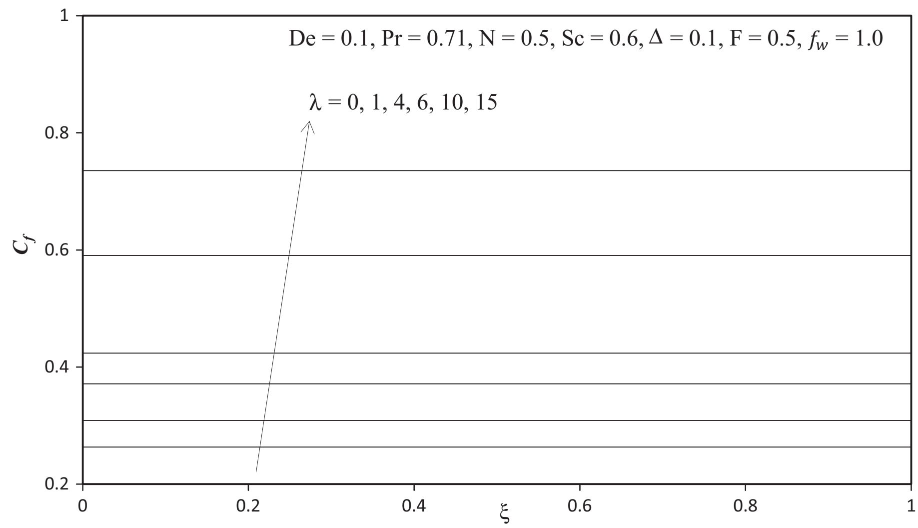

Figure 10a Influence of λ on Local Skin Friction.

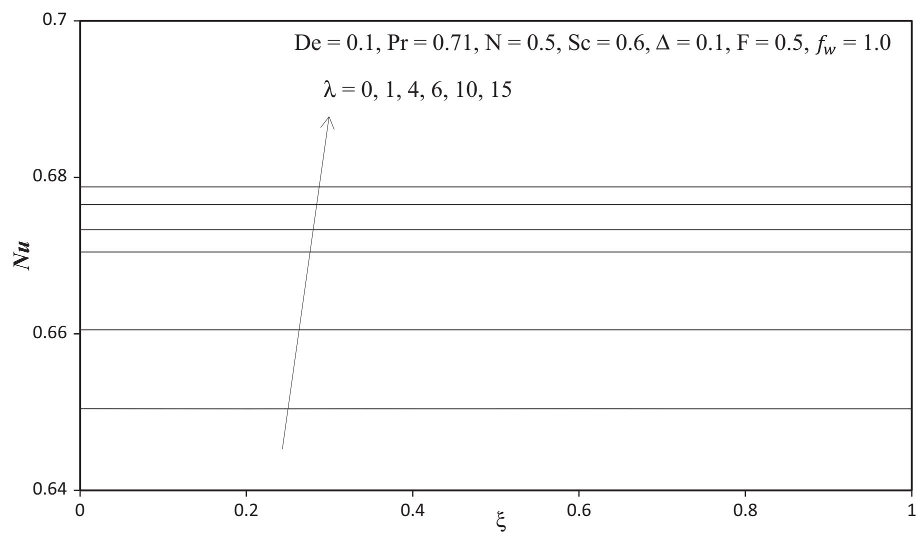

Figure 10b Influence of λ on Nusselt number.

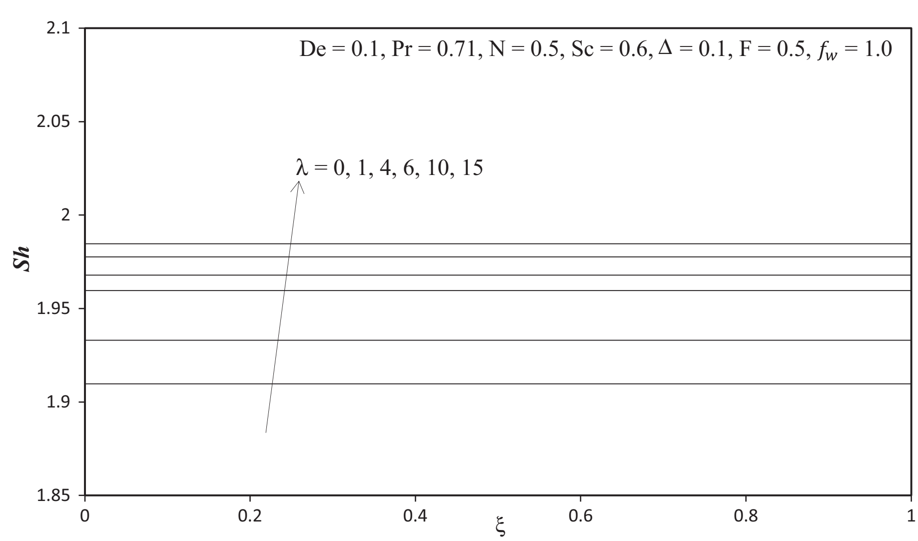

Figure 10c Influence of λ on Sherwood number.

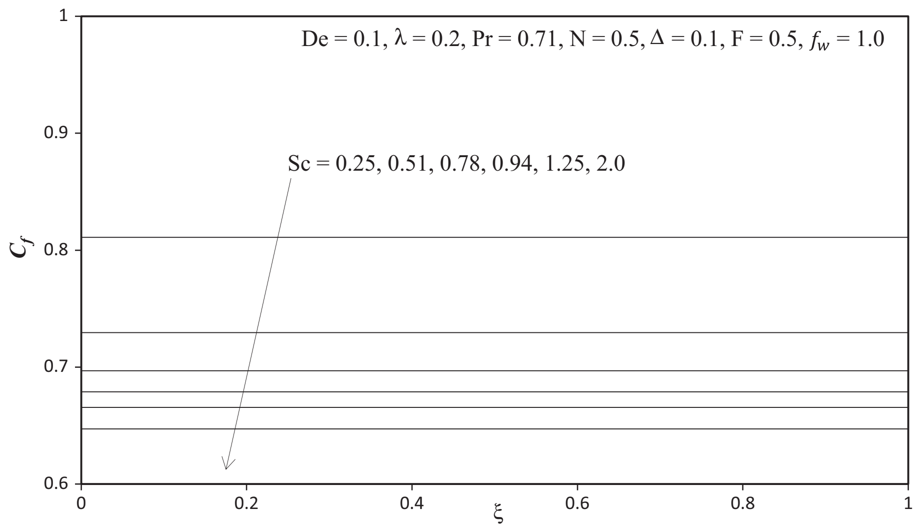

Figure 11a Influence of *Sc* on local skin friction.

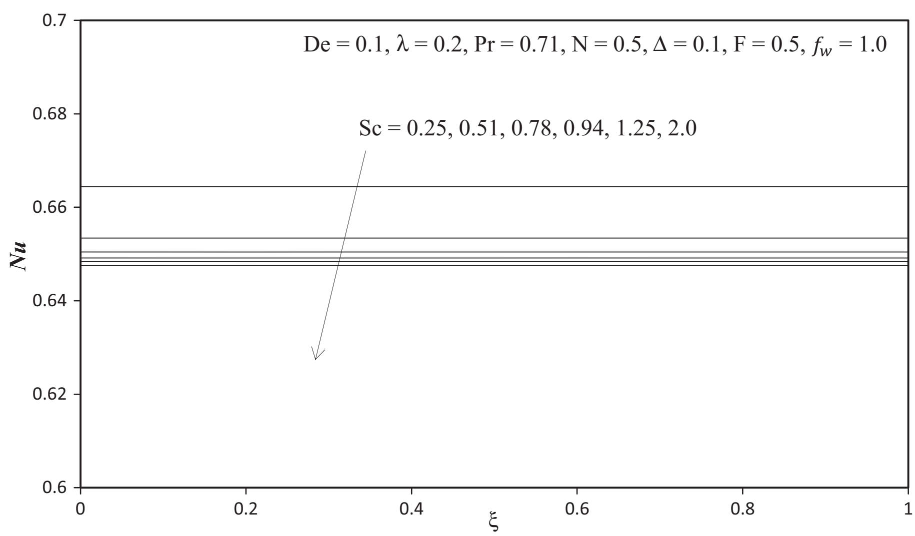

Figure 11b Influence of *Sc* on Nusselt number.

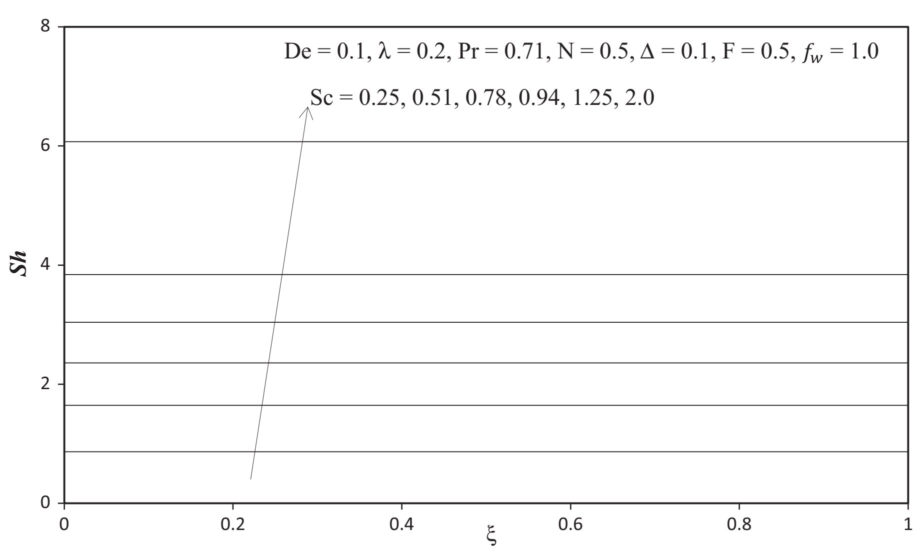

Figure 11c Influence of *Sc* on Sherwood number.

Table 1 Comparison of values of C_f and Nu for different values of F when $De = \lambda = 0$, $Pr = 0.71$, $N = 0.5$, $\Delta = 0.1$, and $f_w = 1.0$.

F	Rao et al. [60]		Present study	
	C_f	Nu	C_f	Nu
0.0	2.1664	0.8365	2.1665	0.8364
0.5	2.4657	0.6139	2.4656	0.6140
1.0	2.6546	0.5032	2.6547	0.5031
2.0	2.9039	0.4010	2.9038	0.4011

decelerated. Further from plate surface there is a transition in the influence of N; $N > 0$ leads to a slight reduction in flow velocity with the contrary for $N < 0$; however, the influence of a large change in N is much less pronounced further from the wall. Buoyance forces therefore exert a much more marked effect in the vicinity of the plate surface. A very different response is sustained by temperature and concentration for different values of N. In both the cases as shown in Figs. 6b and 6c respectively, buoyancy-opposition consistently boosts the values throughout the boundary layer regime. The parameter $N = \frac{\beta^*(C-C_\infty)}{\beta(T-T_\infty)}$ expresses the concentration to thermal buoyancy force ratio. For cases where $N < 1$, thermal buoyancy will dominate concentration buoyancy effects and vice versa for $N > 1$.

Figs. 7a–7c present the profiles for velocity (f'), temperature (θ) and concentration (ϕ) for various values of Schmidt number, Sc. With increasing Sc values from 0.25, the velocity is reduced strongly in the regime. Schmidt number signifies the relative effect of momentum diffusion to species diffusion. For $Sc < 1$, species diffusivity dominates and vice versa for $Sc > 1$, whereas, a slight increase is seen in temperature with increasing Sc values and a strong reduction in concentration is seen with increasing Sc values.

Figs. 8a–8c present the profiles for velocity (f'), temperature (θ) and concentration (ϕ) for various values of Prandtl number, Pr. It is observed that increasing Pr significantly decelerates the flow i.e., velocity decreases throughout the boundary layer regime. The most prominent variation in profiles arises at intermediate distances from the plate surface. Furthermore, increasing Pr generates a substantial reduction in the fluid temperature and the thermal boundary layer thickness. At large Pr, the thermal boundary layer is thinner than at a smaller Pr. This is because for small values of Pr ($Pr \ll 1$), the fluid is highly conductive. Consequently, an increase in Pr decreases the thermal boundary layer thickness. Conversely, an increase in the Pr increases the concentration.

Figs. 9a–9c depict the influence of De, on dimensionless skin friction, heat transfer rate and mass transfer rate at the plate surface. It is observed that the dimensionless skin friction is decreased with the increase in De i.e. the boundary layer flow is decelerated with *greater elasticity effects* in the non-Newtonian fluid. Likewise, the heat transfer rate is also substantially decreased with increasing De values. A decrease in heat transfer rate at the wall will imply less heat is convected from the fluid regime to the plate, thereby heating the boundary layer. The mass transfer rate is also found to be suppressed with increasing De and furthermore plummets with further distance from the lower stagnation point.

Figs. 10a–10c illustrate the response to the parameter ratio of relaxation and retardation times, λ, on the dimensionless skin friction coefficient, heat transfer rate and mass transfer rate at the plate surface. The skin friction at the plate surface is accentuated with increasing λ. Also there is a strong elevation in shear stress (skin friction coefficient) with increasing value of the tangential coordinate, ξ. Heat (local Nusselt number) and mass transfer (local Sherwood number) rates are also increased with increasing, λ.

Figs. 11a–11c present the influence of the Schmidt number, Sc, on the dimensionless skin friction coefficient, heat transfer rate and mass transfer rate at the plate surface. The skin friction at the plate surface is found to be decreasing with increasing Sc. Surface heat transfer rate is also observed to be strongly decreased with increasing Sc values. Mass transfer rate is considerably enhanced with increasing Sc values.

Table 1 presents the comparison values of the present study with those of Rao et al. [60] for different values of thermal radiation, F and are found to be in good correlation.

5. Conclusions

A mathematical model has been developed for the non-similar, buoyancy-driven boundary layer free convection flow, heat and mass transfer of Jeffrey's non-Newtonian fluid past a semi-infinite vertical plate in the presence of thermal radiation and heat generation/absorption. The transformed conservation equations have been solved with prescribed boundary conditions using the implicit finite difference method. A comprehensive assessment of the effects of De, λ, F, Δ, Sc, Pr, f_w and N is made. Very accurate and stable results are obtained with the present finite difference code. The numerical code is able to solve nonlinear boundary layer equations very efficiently and therefore shows excellent promise in simulating transport phenomena in other non-Newtonian fluids. It is therefore presently being employed to study micropolar fluids and viscoplastic fluids which also represent other chemical engineering working fluids. The present study has neglected time effects. Future simulations will also address transient polymeric boundary layer flows and will be presented soon.

References

[1] Anwar Bég O, Abdel Malleque K, Islam MN. Modelling of Ostwald-deWaele non-Newtonian flow over a rotating disk in a non-Darcian porous medium. Int J Appl Math Mech 2012;8:46–67.

[2] Nadeem S, Mehmood Rashid, Akbar Noreen Sher. Thermo-diffusion effects on MHD oblique stagnation point flow of a viscoelastic fluid over a convective surface. Eur Phys J Plus 2014;129:182. http://dx.doi.org/10.1140/epjp/i2014-14182-3.

[3] Prasad VR, Vasu B, Anwar Bég O, Parshad R. Unsteady free convection heat and mass transfer in a Walters-B viscoelastic flow past a semi-infinite vertical plate: a numerical study. Therm Sci-Int Sci J 2011;15(2):291–305.

[4] Tripathi D, Anwar Bég O, Curiel-Sosa J. Homotopy semi-numerical simulation of peristaltic flow of generalized Oldroyd-B fluids with slip effects. Comput Methods Biomech Eng 2014;17 (4):433–42.

[5] Anwar Bég O, Takhar HS, Bharagava R, Prasad VR. Numerical study of heat transfer of a third grade viscoelastic fluid in non-Darcian porous media with thermophysical effects. Phys Scr 2008;77:1–11.

[6] Rashidi MM, Anwar Bég O, Rastegari MT. A study of non-Newtonian flow and heat transfer over a non-isothermal wedge using the homotopy analysis method. Chem Eng Commun 2012;199:231–56.
[7] Huilgol RR, You Z. Application of the augmented Lagrangian method to steady pipe flows of Bingham, Casson and Herschel-Bulkley fluids. J Non-Newton Fluid Mech 2005;128:126–43.
[8] Ramachandra Prasad V, Abdul Gaffar S, Keshava Reddy E, Anwar Bég O. Free convection flow and heat transfer of non-Newtonian tangent hyperbolic fluid from an isothermal sphere with partial slip. Arabian J Sci Eng 2014;39(11):8157–74.
[9] Ramachandra Prasad V, Abdul Gaffar S, Keshava Reddy E, Anwar Bég O. Computational study of non-Newtonian thermal convection from a vertical porous plate in a non-Darcy porous medium with Biot number effects. J Porous Media 2014;17:601–22.
[10] Ramesh GK, Gireesha BJ. Influence of heat source/sink on a Maxwell fluid over a stretching surface with convective boundary conditions in the presence of nanoparticles. Ain Shams Eng J 2014;5(3):991–8.
[11] Jeffreys H. The earth. 4th ed. London: Cambridge University Press; 1929.
[12] Bird RB, Armstrong RC, Hassager O. Dynamics of polymeric liquids. Fluid Dynam, vol. 1. Wiley; 1987.
[13] Kothandapani M, Srinivas S. The effect of heat transfer on the nonlinear peristaltic transport of a Jeffery fluid through a finite vertical porous channel. Int J Biomath 2008;9:915–24.
[14] Nadeem S, Akbar NS. Peristaltic flow of a Jeffery fluid with variable viscosity in an asymmetric channel. Z Naturforsch A 2009;64a:713–22.
[15] Hayat T, Shehzad SA, Qasim M, Obaidat S. Radiative flow of Jeffery fluid in a porous medium with power law heat flux and heat source. Nucl Eng Des 2012;243:15–9.
[16] Vajravelu K, Sreenadh S, Lakshminarayana P, Sucharitha G. The effect of heat transfer on the nonlinear peristaltic transport of a Jeffery fluid through a finite vertical porous channel. Int J Biomath 2008;9, 1650023, 24 pages.
[17] Lakshminarayana P, Sreenadh S, Sucharitha G, Nandgopal K. Effect of slip and heat transfer on peristaltic transport of a Jeffrey fluid in a vertical asymmetric porous channel. Adv Appl Sci Res 2015;6(2):107–18.
[18] Vajravelu K, Sreenadh S, Sucharitha G, Lakshminarayana P. Peristaltic transport of a conducting Jeffrey fluid in an inclined asymmetric channel. Int J Biomath 2014;7(6), 1450064 (25 pages).
[19] Vajravelu K, Sreenadh S, Lakshminarayana P. The influence of heat transfer on peristaltic transport of a Jeffrey fluid in a vertical porous stratum. Commun Nonlinear Sci Numer Simul 2011;16 (8):3107–25.
[20] Akbar Noreen Sher, Ebaid Abdelhalim, Khan ZH. Numerical analysis of magnetic field on eyring-powell fluid flow towards a stretching sheet. J Magn Magn Mater 2015;382:355–8.
[21] Noor NF, Abbasbandy S, Hashim I. Heat and mass transfer of thermophoretic MHD Flow over an inclined radiate isothermal permeable surface in the presence of heat source/sink. Int J Heat Mass Transfer 2012;55:2122–8.
[22] Gupta D, Kumar L, Bég OA, Singh B. Finite element simulation of mixed convection flow of micropolar fluid over a shrinking sheet with thermal radiation. Proc IChemE-Part E, J Process Mech Eng 2014;228(1):61–72.
[23] Cortell, Suction R. Viscous heating and thermal radiation effects on the flow and heat transfer of a power-law fluid past an infinite porous plate. Proc IChemE, Chem Eng Res Design 2011;89:85–93.
[24] Bhargava R, Sharma R, Bé g OA. A numerical solution for the effect of radiation on micropolar flow and heat transfer past a horizontal stretching sheet through a porous medium. In: 7th SWEAS int. conf. on heat mass transfer (HMT'10). UK: University of Cambridge; 2010. p. 88–96.
[25] Akbar NS, Khan ZH, Haq RU, Nadeem S. Dual solutions in MHD stagnation-point flow of a Prandtl fluid impinging on a shrinking sheet. Appl Math Mech 2014;35(7):813–20.
[26] Pohlhausen H. Der warmeaustrausch zwischen festen korpen und flussigkeiten mit kleiner reibng und kleiner warmeleitung. ZAMM 1921;1:115–21.
[27] Ostrach S. An analysis of laminar free convection flow and heat transfer along a flat plate parallel to the direction of the generating body force. NACA Report 1111; 1953.
[28] Jaluria Y. Natural convection heat and mass transfer. Oxford: Pergamon Press; 1980.
[29] Merkin JH. The effect of buoyancy forces on the boundary layer flow over semi-infinite vertical flat plate in a uniform free stream. J Fluid Mech 1969;35:439–50.
[30] Lloyd JR, Sparrow EM. Combined forced and free convection flow on vertical surfaces. Int J Heat Mass Transfer 1970;13:434–8.
[31] Wilks G. Combined forced and free convection flow on vertical surfaces. Int J Heat Mass Transfer 1973;16:1958–64.
[32] Takhar HS, Chamkha AJ, Nath G. Unsteady flow and heat transfer on a semi-infinite flat plate with an aligned magnetic field. Int J Eng Sci 1999;37:1723–36.
[33] Hossian MA, Ahmed M. MHD forced and free convection boundary layer near the leading edge. Int J Heat Mass Transfer 1990;33(3):571–5.
[34] Takhar HS, Chamkha AJ, Gorla RSR. Combined convection-radiation interaction along a vertical flat plate in a porous medium. Int J Fluid Mech Res 2005;32:139–56.
[35] Sparrow EM, Cess RD. Free convection with blowing or suction. J Heat Transfer 1961;83:387–96.
[36] Merkin JH. Free convection with blowing and suction. Int J Heat Mass Transfer 1972;15:989–99.
[37] Clarke JF. Transpiration and natural convection: the vertical flat plate problem. J Fluid Mech 1973;57:45–61.
[38] Merkin HJ. The effects of blowing and suction on free convection boundary layers. Int J Heat Mass Transfer 1975;18:237–44.
[39] Vedhanayagam M, Altenkirch RA, Eichhorn R. A transformation of the boundary layer equations for the free convection past a vertical flat plate with arbitrary blowing and suction wall temperature variations. Int J Heat Mass Transfer 1980;23:1286–8.
[40] Clarke JF, Riley N. Free convection and the burning of a horizontal fuel surface. J Fluid Mech 1976;74:415–31.
[41] Lin HT, Yu WS. Free convection on a horizontal plate with blowing and suction. Trans ASME J Heat Transfer 1988;110:793–6.
[42] Chamkha AJ. Non-similar solutions for heat and mass transfer by hydromagnetic mixed convection flow over a plate in porous media with surface suction or injection. Int J Numer Meth Heat Fluid Flow 2000;10:142–62.
[43] Chamkha AJ, Abd El-Aziz MM, Ahmed SE. Effects of thermal stratification on flow and heat transfer due to a stretching cylinder with uniform suction/injection. Int J Energy Technol 2010;2:1–7.
[44] Chamkha AJ, Aly AM, Mansour MA. Similarity solution for unsteady heat and mass transfer from a stretching surface embedded in a porous medium with suction/injection and chemical reaction effects. Chem Eng Commun 2010;197:846–58.
[45] Anwar Hossain M, Khanafer K, Vafai K. The effect of radiation on free convection flow with variable viscosity from a porous vertical plate. Int J Therm Sci 2001;40:115–24.
[46] Sturdza P. An aerodynamic design method for supersonic natural laminar flow aircraft PhD thesis. California, USA: Dept. Aeronautics and Astronautics, Stanford University; 2003.
[47] Bird RB, Armstrong RC, Hassager O. Dynamics of polymeric liquids. Fluid mechanics, vol. 1. New York: Wiley; 1977.
[48] Gorla RSR. Radiative effect on conjugate forced convection in a laminar wall jet along a flat plate. Encyclopedia fluid mechanics. Suppl. 3: Advances in flows dynamics. Texas, USA: Gulf Publishing; 1993.

[49] Bég, Anwar O, Zueco J, Ghosh SK, Heidari A. Unsteady magnetohydrodynamic heat transfer in a semi-infinite porous medium with thermal radiation flux: analytical and numerical study. Adv Numer Anal 2011;2011, 17 pages Article ID 304124.
[50] Keller HB. Numerical methods in boundary-layer theory. Ann Rev Fluid Mech 1978;10:417–33.
[51] Anwar Bég O. Numerical methods for multi-physical magnetohydrodynamics. New developments in hydrodynamics research. New York: Nova Science; 2012. p. 1–112 [chapter 1].
[52] Lok YY, Pop I, Ingham DB. Oblique stagnation slip flow of a micropolar fluid. Meccanica 2010;45:187–98.
[53] Chang T-B, Mehmood A, Anwar Bég O, Narahari M, Islam MN, Ameen F. Numerical study of transient free convective mass transfer in a Walters-B viscoelastic flow with wall suction. Comm Nonlinear Sci Numer Simul 2011;16:216–25.
[54] Srinivasacharya D, Kaladhar K. Mixed convection flow of couple stress fluid in a non-Darcy porous medium with Soret and Dufour effects. J Appl Sci Eng 2012;15:415–22.
[55] Abdul Gaffar S, Ramachandra Prasad V, Anwar Bég O. Computational analysis of magnetohydrodynamic free convection flow and heat transfer of non-Newtonian tangent hyperbolic fluid from a horizontal circular cylinder with partial slip. Int J Appl Comput Math 2015;1(4):651–75.
[56] Prasad VR, Gaffar SA, Anwar Bég O. Heat and mass transfer of a nanofluid from a horizontal cylinder to a micropolar fluid. AIAA J Thermophys Heat Transfer 2015;29:127–39.
[57] Darji RM, Timol MG. On invariance analysis of MHD boundary layer equations for non-Newtonian Williamson fluids. Int J Adv Appl Math Mech 2014;1:10–9.
[58] Singh V, Agarwal S. Flow and heat transfer of Maxwell fluid with variable viscosity and thermal conductivity over an exponentially stretching sheet. Am J Fluid Dynam 2013;3:87–95.
[59] Nadeem S, Mehmood Rashid, Akbar Noreen Sher. Non-orthogonal stagnation point flow of a nano non-Newtonian fluid towards a stretching surface with heat transfer. Int J Heat Mass Transf 2013;57(2):679–89.
[60] Rao VS, Baba LA, Raju RS. Finite element analysis of radiation and mass transfer flow past semi-infinite moving vertical plate with viscous dissipation. J Appl Fluid Mech 2013;6(3):321–9.

S. Abdul Gaffar was born in Madanapalle, Chittoor District, Andhra Pradesh, India, in May, 1982. He obtained a First Class Masters of Sciences, degree in Mathematics (2004) from Sri Venkateswara University, Tirupati, and is pursuing Ph.D. in Flow and Heat transfer of Casson Fluid on Boundary Layer (Registered in 2011), JNT University Anantapur, Anantapuramu. He worked as lecturer in the Department of Mathematics, Bapatla College of Engineering, India, for one year (2004). Later from May 2007 to April 2013, he was the Assistant Professor for five years in the Department of Mathematics, Mother Theresa Institutions. From 2013 to till date he is working as Lecture in the Department of Mathematics, Salalah College of Technology, Salalah, OMAN. He has published in excess of 14 journals in peer reviewed journals. He is currently engaged in different non-Newtonian fluids over different curved bodies.

V. Ramachandra Prasad was born in Madanapalle, Chittoor District, Andhra Pradesh, India, in July, 1968. He obtained a Distinction Class Masters of Sciences, degree in Mathematics (1994) from Osmania University, Hyderabad, and a Ph.D. in Radiation and Mass Transfer Effects on connective flow past a vertical plate (2003), both from Sri Venkateswara University, Tirupati. He then worked as lecturer in the Department of Mathematics, Besant Theosophical College, Madanapalle, India, for seven years (1994–2001). From May 2001 to April 2007, he was the Assistant Professor for six years in the Department of Mathematics, in Madanapalle Institute of Technology and Science. Later from May 2007 to April 2009 worked as Associate Professor, in the Department of Mathematics, Madanapalle Institute of Technology and Science, Madanapalle, India. Form May 2009 to till date he is working as Professor in the Department of Mathematics, Madanapalle Institute of Technology and Science, Madanapalle, India. He has authored Radiation effects on Convective Flow Past a Vertical Plate: Radiation and Mass Transfer Effects on Convective Flow Past a Vertical Plate, *(Lambert, Germany, 2010), Thermo-Diffusion and Diffusion-Thermo Effects on Boundary Layer Flows (Lambert, Germany, 2011) and Walters_B Viscoelastic flow Past a Vertical Plate:Numerical Study of Unsteady Free Convective Heat and Mass Transfer in a Walters_B Viscoelastic Flow Past a Vertical Plate (Lambert, Germany, 2012)*. He has published in excess of 50 journal articles. His research has also been presented at over 13 conferences. He is currently engaged in different non-Newtonian fluids over different curved bodies.

E. Keshava Reddy, presently working as Professor of Mathematics in JNT University College of Engineering Anantapur. He has 15 years of experience in teaching and 11 years in research. He obtained his Ph.D. degree in Mathematics from prestigious University (Banaras Hindu University, Varanasi). His areas of interest include Functional Analysis, Optimization Techniques, Data Mining, Neural Networks, Fuzzy Logic and Optimization techniques. He guided 2 Ph.D., 1 M.Phil. and has published more than 35 Research papers in National and International Journals and Conferences. He authored 6 books on Engineering Mathematics and Mathematical Methods for various universities. He worked as Chairman of Board of Studies for the faculty of Mathematics for JNTUA at both UG level and PG level. Presently he is the chairman of PG Board of Studies for Mathematics of JNTUA. He is a member of Board of Studies for Mathematics of various universities.